Available online at www.sciencedirect.com
SCIENCE DIRECT®
Journal of Nuclear Materials 337–339 (2005) 580–584
journal of nuclear materials
www.elsevier.com/locate/jnucmat

Multi-scale modeling of hydrogen isotope transport in porous graphite

M. Warrier [a,*], R. Schneider [a,*], E. Salonen [b], K. Nordlund [c]

[a] Max-Planck-Institut für Plasmaphysik, EURATOM Association, D-17491 Greifswald, Germany
[b] Laboratory of Physics, HIP, P.O. Box 1100, FIN–02015 HUT, Finland
[c] Accelerator laboratory, P.O. Box 43, FIN–00014, University of Helsinki, Finland

Abstract

We present a multi-scale model for hydrogen isotope transport in graphite. We use molecular dynamics (MD) simulations to study hydrogen isotope transport in a graphite micro-crystal which is a few nanometers in size. The MD results are parametrized in a Kinetic Monte Carlo (KMC) model as a diffusion process of two competing thermally activated events. Micro-crystal diffusion coupled with a trapping–detrapping model at microvoids has then been used in a KMC model to simulate diffusion across a granule which is typically a few microns in size. Finally we extend these models to the centimeter scale and present initial results for hydrogen isotope transport in 3d, porous graphite.

PACS: 02.70.Ns; 02.70.Lq; 66.30.−h; 66.30.Ny
Keywords: Graphite; Hydrogen inventory; Multi-scale modeling

1. Introduction

The graphite used in fusion devices as first wall material is porous and consists of granules and voids. These granules are typically a few microns across and are separated by voids which are typically a fraction of a micron in size. The granules further consist of graphitic microcrystallites of size equal to a few nm and separated by microvoids of typically a fraction of a nm (Fig. 1) [1–4]. Therefore there exists a large internal surface area bounding the granules and also within the granules bounding the crystallites. It is estimated that the trap site concentrations within the graphite bulk are of the order 10^{-3}–10^{-5} per C atom [5,6]. Graphites exposed to fusion edge plasmas also get damaged by the incident energetic ions and neutrals from the plasma resulting in a high density of trap sites within the range of penetration of the incident ions ([2,5] and references therein).

Therefore the incident hydrogen ions and neutrals which are not reflected at the surface have a wide range of possibilities as discussed in [1–3,7]. They can

- get trapped either in the region with a high density of traps or in the bulk and
  - become detrapped, or
  - undergo chemical reactions to form hydrocarbons or recombine to form hydrogen molecules which can then diffuse along microvoids or voids.
- be solute and
  - become trapped, or

* Corresponding authors.
E-mail addresses: manoj.warrier@ipp.mpg.de (M. Warrier), ralf.schneider@ipp.mpg.de (R. Schneider).

0022-3115/$ - see front matter © 2004 Elsevier B.V. All rights reserved.
doi:10.1016/j.jnucmat.2004.10.017

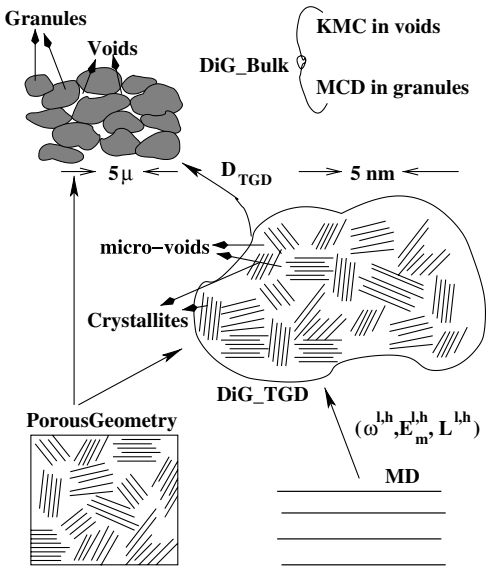

Fig. 1. Multi-scale schematic.

- diffuse within the crystallites, or
- diffuse along the crystallite surfaces, or
- recombine to form molecules at the crystallite surfaces (or granule surfaces) and undergo diffusion along the microvoids (or voids).

The existence of such large variations in length scales of the sub structures, coupled with the wide range of possible atomistic processes, makes the study of hydrogen transport and inventory (or complementing this, the formation of hydrocarbons and their transport) in graphite a non-trivial exercise. Many detailed macroscopic models have been proposed to study hydrogen isotope inventory and transport in porous graphite [1–4] and hydrocarbon formation and transport in graphite [8]. These models use rate constants for transport from experiments [7,9–13], some of which still need theoretical explanations. On the other hand, there exists microscopic models [14–17] using molecular dynamics (MD) with either empirical potentials or density functional theory which have given insight into the microscopic mechanisms in graphite. It is desirable to use the insights gained from the microscopic models in modeling the transport in the meso-scale and further in the macroscale in order to understand the physical processes contributing to macroscopic transport.

We have earlier modeled hydrogen isotope diffusion in pure, crystalline graphite using MD at micro-scales (2.5 nm, 10^{-10} s) and parametrized a kinetic Monte Carlo (KMC) scheme from the MD results [17]. A 3d, porous, granule structure was constructed using statistical distributions for crystallite dimensions and crystallite orientations for a specified microvoid fraction. The KMC scheme was extended to include trapping and detrapping at the crystallite–microvoid interface in the 3d porous granule structure to simulate trans-granular diffusion (TGD) in the meso-scales (10^{-7}–10^{-6} m, ms) [18] using the results from our micro-scale modeling and from experiments ([19] and references therein). In this paper we first present simple models which reproduce the results of our simulations at the micro and meso scales. We then describe a scheme by which we extend our simulations to the macro-scale (1 cm, up to a few s), thereby having a truly multi-scale capability. Finally, we present the first results from our simulations at the macro-scales.

2. Simple model for H isotope transport in crystal graphite

Molecular dynamics simulations using the `HCParcas` code were carried out to study the diffusion of hydrogen isotopes in crystalline graphite in the temperature range 150–900 K. It was seen that the diffusion is non-Arrhenius-like, but could be described as a sum of two types of thermally activated mechanisms; one with a low jump attempt frequency ω_o ($\omega_o^l = 6.8 \times 10^{12}/\sqrt{m}\,\mathrm{s}^{-1}$, where m is the isotope mass in amu), and a low activation energy E_m ($E_m^l = 0.0148$ eV) and another with a higher ω_o ($\omega_o^h = 2.74 \times 10^{13}\,\mathrm{s}^{-1}$) and higher E_m ($E_m^h = 0.27$ eV) [18]. This parametrization of the diffusion $(\omega_o^{l,h}, E_m^{l,h}, L^{l,h})$, where $L^{l,h}$ is the distance jumped at low frequency (superscript l) and high frequency (superscript h) jumps, used as input in the KMC code `DiG` qualitatively and quantitatively reproduces the MD results [17]. No diffusion events across the graphene layers were observed in the temperature range studied.

2.1. Model

Based on the above results we formulate a simple model for the diffusion of a particle that gets trapped with two possible trap energies E_m^l and E_m^h. The particle attempts to jump out of the traps with frequencies ω_o^l and ω_o^h. It is assumed that the jumps are Poisson-like processes. The two types of jumps occur with a typical frequency of $\omega^{l,h} = \omega_o^{l,h} \mathrm{e}^{\frac{-E_m^{l,h}}{k_B T}}$ (where $k_B T$ is the crystallite temperature in eV). The probability of a jump of length $L^{l,h}$ occurring is given by $P^{l,h} = \frac{\omega^{l,h}}{\omega^l + \omega^h}$. Assuming a simple random walk in two dimensions (in-between the graphene planes), the mean square displacement after N steps is

$$\langle (R(t) - R(0))^2 \rangle = N(P^l [L^l]^2 + P^h [L^h]^2), \quad (1)$$

where $R(t)$ is the position vector of the particle at a given time t. The time increment for each jump event is given by [20]

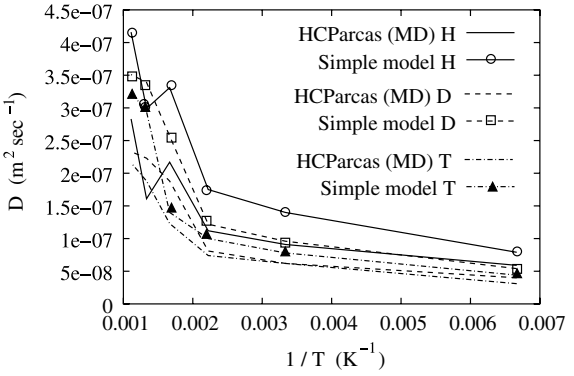

Fig. 2. Comparison of model with MD results for hydrogen transport in crystal graphite.

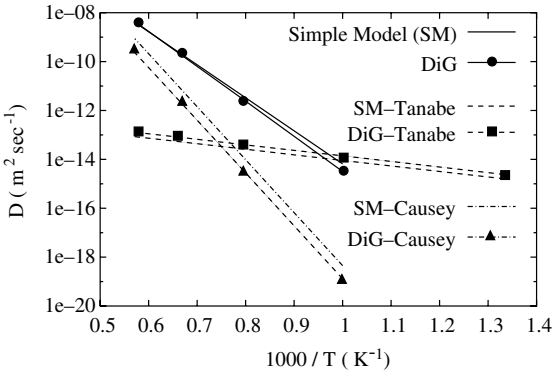

Fig. 3. Comparison of TGD coefficients from the simple model (SM) with simulation results (DiG). [18]

$$\Delta t = -\frac{\ln(U)}{\omega^l + \omega^h}, \tag{2}$$

where U is a uniform random number between 0 and 1, and assuming that the jumps are independent events. Therefore from Eqs. (1) and (2), we get the diffusion coefficient of a hydrogen isotope in crystalline graphite as

$$D = \frac{1}{2d}\frac{\langle (R(t) - R(0))^2 \rangle}{\Delta t} = \frac{N}{4}\frac{\omega_o^l e^{\frac{-E_m^l}{k_B T}}(L^l)^2 + \omega_o^h e^{\frac{-E_m^h}{k_B T}}(L^h)^2}{\sum_i^N(-\ln(U_i))}, \tag{3}$$

where $d = 2$ is the dimensionality of the random walk. Using the parameters $(\omega_o^{l,h}, E_m^{l,h})$ as described above and a value of 10 Å for L^h, and 3.8 Å for L^l in Eq. (3), we obtain a good quantitative and qualitative match with the MD results (Fig. 2). Note that L^l was chosen to be (i) 4.8 Å at 600 K for hydrogen, (ii) 5 Å at 600 K and at 750 K for deuterium and (iii) 4.5 Å at 600 K and 5 Å at 750 K for tritium. These modified values of L^l are used to match the MD results which show enhanced diffusion of the hydrogen isotopes at these specific temperatures [17,18].

3. Simple model for TGD

In order to simulate TGD, a porous granule structure with randomly oriented crystallites and microvoids was created and a trapping–detrapping model at the crystallite–microvoid interfaces was implemented in the KMC algorithm `DiG` [18]. Based on the results of the simulations, we assume (i) that the crystallite diffusion times are negligible, which is valid for H isotopes in pure crystal graphite and (ii) isotropic 3d diffusion. This is valid since as the particle traverses the granule it encounters crystallites having a random orientation and also the microvoid diffusion paths or the grain diffusion in-between the crystallites allows 3d random motion.

Using these assumptions we get the trans-granular diffusion coefficient to be

$$D_{\mathrm{TGD}} = \frac{N}{6}\left(\frac{P^{\mathrm{void}}(L^{\mathrm{void}})^2 + P^{\mathrm{cryst}}(L^{\mathrm{cryst}})^2}{\sum_{i=1}^N(-\ln(U_i))}\right)\omega^{\mathrm{detrap}}, \tag{4}$$

where N is the number of steps in the random walk, and L^{void} and L^{cryst} are the step sizes of the random walk in a void and in the crystallite respectively. P^{void} and P^{cryst} are the probabilities of the detrapped particle getting into a void or into a crystallite. ω^{detrap} is the detrapping frequency given by $\omega_o^{\mathrm{detrap}} e^{\frac{-E_m^{\mathrm{detrap}}}{k_B T}}$, where $\omega_o^{\mathrm{detrap}}$ is the detrap attempt frequency, E_m^{detrap} is the detrapping energy and T is the target temperature.

With this simple model we are able to reproduce the results from our TGD modeling (Fig. 3) [18], which matches the experimental results [19]. From this modeling additional information on the graphite structure properties, such as microvoid sizes and crystallite sizes can be obtained.

4. Scaling up to centimeters

The scaling up method is illustrated in Fig. 1. The block labeled **PorousGeometry** is used to create both, the granule with crystallites and microvoids (**DiG_TGD**) and the bulk graphite (**DiG_Bulk**). Note that these two are similar structures except that in the **DiG_TGD** case crystallite orientations also need to be specified. Parametrization of the **MD** results to do TGD at the meso-scales has been briefly described above and in detail in [17,18].

We initially create a cubic granular structure with a side length 5×10^{-3} cm which typically accommodates 8000 granules. In order to extend the granular geometry to centimeter scales, we apply periodic boundary

conditions along the X and Y directions which are the directions parallel to the graphite surface. Along the Z direction which lies perpendicular to the graphite surface, we replicate the structure only in one direction ($Z > 0$). The graphite surface lies at $Z = 0$, and particles reaching this have a probability of being desorbed. The desorption event is handled by the KMC algorithm. The KMC algorithm also takes care of transport within the voids and void-granule surfaces. A Monte Carlo diffusion algorithm [21] is implemented within the granules with the diffusion coefficient for TGD, D_{TGD}, obtained from the simulations of TGD at the meso-scales.

4.1. First results

We consider a case of only 1000 H atoms uniformly distributed in the X–Y plane. The atoms have a Gaussian distribution along the Z axis, centered at a depth of 100 Å from the surface with a width 10 Å. The void fraction was chosen to be 0.1 and therefore most of the particles end up inside granules. The rest of the particles are assumed to be solute H on the void-granule interface. Due to the low concentration of H atoms, hydrogen molecules are not formed. The results are applicable to a very low concentration case. However this calculation gives an idea of possible transport preferences within the various regions, i.e. voids, granules and out of the surface (recycling).

The inputs to the code can be from a mixture of experimental results and MD simulations. The activation energy for trapping–detrapping within the granule is taken to be 2.7 eV since the TGD diffusion coefficient obtained from our simulations using this value lies nicely in the middle of the range reported in experiments [19]. Within the KMC algorithm, the activation energy for desorption is taken to be 1.91 eV [22]. The activation energy for surface diffusion is taken to be 0.9 eV, with a jump attempt frequency of $10^{13}\,s^{-1}$ and a jump step length of 34.64 Å to match the surface diffusion coefficient reported in [6]. Activation energy for entering the surface for a solute H atom is same as the activation energy for TGD. The simulations are carried out at target temperatures between 300 and 1500 K in intervals of 300 K and the final number of particles in different regions are plotted as a function of target temperature (Fig. 4). In this plot N stands for the number of particles in a region and the region is given as a subscript. We see that there is almost no transfer of particles from one region to another below 900 K because the activation energies for bulk diffusion and desorption are too high. Most of the transport is by surface diffusion of the solute atoms. Particles start getting into the bulk and from the bulk to the voids in our simulations at 1200 K and this is more pronounced at 1500 K. It is also seen that H atom recycling starts off above 900 K. Such behavior is observed in experiments [6,23].

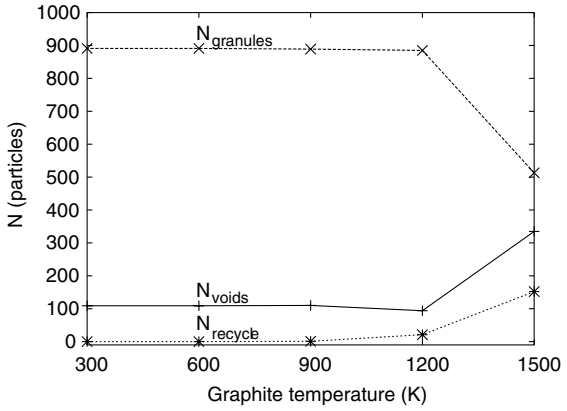

Fig. 4. Number of particles in different regions at the end of a million KMC steps.

5. Summary and conclusions

We have devised a multi-scale scheme to model hydrogen transport in porous graphite. First results from this scheme are in good agreement with current understanding of H transport in graphite, as well as with experimental data. We have also developed simple models that match our simulations at the micro-scales and meso-scales. It must be emphasized that in pursuing the aim of scaling up the calculations, both in time and the system size, we have neglected many effects at the microscopic and mesoscopic scales, such as diffusion in a damaged crystallite, existence of carbon atoms in sp^3 hybridized states and bonds at the crystallite–microvoid interface region, re-entry probability of H isotopes into the crystallites, etc. This is not because these aspects are unimportant or uninteresting, but only because the aim of this study is to show a means of relating macroscopic transport to microscopic effects by constructing a multi-scale modeling hierarchy. By doing this it also becomes obvious what aspects at the micro-scales and meso-scales need to be studied in more detail. The extension of the model by including additional effects like (i) using pseudo-particles to handle fusion relevant fluxes, (ii) multiple species and (iii) chemical reactions is planned for the future. These effects are not difficult to implement because of the modular way the code is being developed.

Acknowledgments

M. Warrier would like to thank a host of researchers from the materials science group at IPP-Garching for their comments and Dr Alexej Runov for an introduction to Monte Carlo diffusion.

References

[1] W. Möller, J. Nucl. Mater. 162–164 (1989) 138.
[2] A.A. Haasz et al., J. Appl. Phys. 77 (1) (1995) 66.
[3] G. Federici, C.H. Wu, J. Nucl. Mater. 186 (1992) 131.
[4] A. Hassanein, B. Wiechers, I. Konkashbaev, J. Nucl. Mater. 258–263 (1998) 295.
[5] M. Mayer, M. Balden, R. Behrisch, J. Nucl. Mater. 252 (1998) 55.
[6] R.A. Causey, M.I. Baskes, K.L. Wilson, J. Vac. Sci. Technol. A 4 (3) (1986) 1189.
[7] J. Küppers, Surface Sci. Rep. 22 (1995) 249.
[8] B.V. Mech, A.A. Haasz, J.W. Davis, J. Appl. Phys. 84 (3) (1998) 1655.
[9] B.M.U. Scherzer et al., Nucl. Instrum. and Meth. B 33 (1988) 714.
[10] B.M.U. Scherzer, J. Wang, W. Möller, J. Nucl. Mater. 162–164 (1989) 1013.
[11] W. Möller, B.M.U. Scherzer, J. Appl. Phys. 64 (1988) 4860.
[12] R.A. Causey, J. Nucl. Mater. 162–164 (1989) 151.
[13] H. Atsumi, S. Tokura, M. Miyake, in: Proc. 3rd Int. Conf. on Fusion Reactor Materials, Karlsruhe, 1987; H. Atsumi, S. Tokura, M. Miyake, J. Nucl. Mater. 155–157 (1988) 241.
[14] E. Salonen, K. Nordlund, J. Keinonen, C.H. Wu, Phys. Rev. B 63 (2001) 195415.
[15] Y. Ferro, F. Marinelli, A. Allouche, Chem. Phys. Lett. 368 (2003) 609.
[16] Y. Ferro, F. Marinelli, A. Allouche, J. Chem. Phys. 116 (18) (2002) 8124.
[17] M. Warrier, R. Schneider, E. Salonen, K. Nordlund, Phys. Scr. T 108 (2004) 85.
[18] M. Warrier, R. Schneider, E. Salonen, K. Nordlund, Contrib. Plasma Phys. 44 (1–3) (2004) 307.
[19] K.L. Wilson et al., J. Nucl. Fusion 1 (1991) 31.
[20] K.A. Fichthorn, W.H. Weinberg, J. Chem. Phys. 95 (2) (1991) 1090.
[21] P.E. Kloeden, E. Platen, Numerical solution of stochastic differential equations, Springer series in Applications of Mathematics, vol. 23, 1999.
[22] K. Ashida, K. Ichimura, M. Matsuyama, K. Watanabe, J. Nucl. Mater. 128 (129) (1984) 792.
[23] P. Franzen, E. Vietzke, J. Vac. Sci. Technol. A 12 (3) (1994) 820.